

REPORT DOCUMENTATION PAGE			Form Approved OMB No. 0704-0188	
Public reporting burden for this collection of information is estimated to average 1 hour per response, including the time for reviewing instructions, searching existing data sources, gathering and maintaining the data needed, and completing and reviewing the collection of information. Send comments regarding this burden estimate or any other aspect of this collection of information, including suggestions for reducing this burden, to Washington Headquarters Services, Directorate for Information Operations and Reports, 1215 Jefferson Davis Highway, Suite 1204, Arlington, VA 22202-4302, and to the Office of Management and Budget, Paperwork Reduction Project (0704-0188), Washington, DC 20503.				
1. AGENCY USE ONLY (Leave Blank)	2. REPORT DATE 31 October 1996	3. REPORT TYPE AND DATES COVERED Professional Paper		
4. TITLE AND SUBTITLE  Optical Biasing of Ring Laser Gyroscope by Quantum Well Mirror		5. FUNDING NUMBERS		
6. AUTHOR(S)  Francis A. Karwacki, Martin A. Sanzari, Luigi Greco Zameer Hasan, H. L. Cui and J. E. Cunningham				
7. PERFORMING ORGANIZATION NAMES(S) AND ADDRESS(ES) COMMANDER NAVAL AIR WARFARE CENTER AIRCRAFT DIVISION 22541 MILLSTONE ROAD PATUXENT RIVER, MD 20670-5304		8. PERFORMING ORGANIZATION REPORT NUMBER		
9. SPONSORING / MONITORING AGENCY NAME(S) AND ADDRESS(ES) Office of Naval Research (331) 800 Quincy Street Arlington, VA 22217-5660		10. SPONSORING / MONITORING AGENCY REPORT NUMBER		
11. SUPPLEMENTARY NOTES				
12a. DISTRIBUTION / AVAILABILITY STATEMENT  APPROVED FOR PUBLIC RELEASE: DISTRIBUTION UNLIMITED		12b. DISTRIBUTION CODE		
13. ABSTRACT (Maximum 200 words) The Quantum Well Mirror (QWM) is a semiconductor device fabricated from AlGaAs/AlAs. It is composed of two structures, a back surface mirror and a front filter. The purpose of the QWM is to optically bias the ring gyroscope (RLG) out of the lock-in region. This is accomplished by shifting the apparent plane of reflection within the QWM by applying a voltage to the electrodes which control the optical filter. This device will reduce cost of the RLG by *Removal of the mechanical dither hinge assemblies * Removal of the high voltage circuitry used to drive the dither hinge *Removal of the path-length controller assemblies. *Loosening of the performance requirement for the inertial sensor assembly (ISA) shock mounts. *Increased reliability resulting from the removal of all mechanical assemblies in the RLG system.				
Subject Terms OPTICAL BIASING RING LASER GYROSCOPE QUANTUM WELL MIRROR SEMICONDUCTOR DEVICE		DTIC QUALITY INSPECTED 4		15. NUMBER OF PAGES  23
				16. PRICE CODE
17. SECURITY CLASSIFICATION OF REPORT  UNCLASSIFIED	18. SECURITY CLASSIFICATION OF THIS PAGE  UNCLASSIFIED	19. SECURITY CLASSIFICATION OF ABSTRACT  UNCLASSIFIED	20. LIMITATION OF ABSTRACT  N/A	

19961211 054

**Francis A. Karwacki**

Naval Air Warfare Center, AirCRAFT Division, Patuxent River, MD 20670-5304

**Martin A. Sanzari and Luigi Greco**

Department of Physics, Fordham University, Bronx, NY 10458

**Zameer Hasan**

Department of Physics, Temple University, Philadelphia, PA

**H.L. Cui**

Department of Physics, Stevens Institute of Technology, Hoboken, NJ 07030

**J.E.**

**Robert Cunningham**

Lucent Technology, Murray Hill, NJ

### **Optical Biasing of a Ring Laser Gyroscope by a Quantum Well Mirror**

An novel optical biasing technique for the Laser Gyroscope (RLG) will be discussed. Included in the discussion will be the optical biasing technique, the device structure and available experimental data.

## Introduction

The Quantum Well Mirror (QWM) is a semiconductor device fabricated from AlGaAs/AlAs. It is composed of two structures, a back surface mirror and a front surface filter. The purpose of the QWM is to optically bias the ring laser gyroscope (RLG) out of the lock-in region. This is accomplished by shifting the apparent plane of reflection within the QWM by applying a voltage to the electrodes which control the optical filter. This device will reduce the cost of the RLG by

- \* Removal of the mechanical dither hinge assemblies.
- \* Removal of the high voltage circuitry used to drive the dither hinge.
- \* Removal of the path-length controller assemblies.
- \* Loosening of the performance requirement for the inertial sensor assembly (ISA) shock mounts.
- \* Increased reliability resulting from the removal of all mechanical assemblies in the RLG system.

In addition, a reduction in random walk error will result from higher dither drive frequencies. The dither contribution to the random walk of the gyro is given by:

$$RW = \frac{\omega_L}{\sqrt{SF 2 \pi \omega_d}} \quad (1)$$

where  $\omega_L$  is the lock-in frequency of the gyro and SF is the Scale Factor. A typical body-dithered RLG has a dither frequency of 350-500 Hz. An electro-optically modulated semiconductor structure can easily attain a modulation frequency of 100 MHz. For an increase in the dither frequency from 375 Hz to 100 MHz, the random walk induced by dither is decreased by a factor of 516. This potentially decreases the random walk of the gyroscope to the quantum limit.

## Operational Principle

The QWM provides an optical bias by moving its apparent plane of reflection back and forth. This is similar to moving the position of the corner mirrors back and forth using a piezoelectric device. A simple analysis of the motion and can be performed using Figure 1. In this configuration a rectangular RLG cavity is assumed for simplicity. The first step is to move the dither motion to the mirrors. Instead of rotating the gyro body back and forth, we move the mirrors in and out. Opposing mirrors move 180 degrees out of phase with each other. This action produces an equivalent rotation which can be derived as follows:

Considering an optical measurement, where light  $E_i$  at  $\omega_o$  (in the lab frame) is injected into the cavity through one partially transmitting mirror as shown in Figure 1. The change in cavity length with mirror motion (away from equilibrium position) will be observable as a phase shift. This phase shift occurs between the light which makes a round trip in the cavity and passes out through the injection mirror  $E_i$  with the fraction of the input wave that is reflected from the input mirror  $E_r$ . Multiple passes are ignored for now since the combination of a series of transmitted waves would change the net phase measured, so this is an approximation for low mirror reflectivity. The question of multiple-pass phase measurement becomes moot if one considers changing the input frequency to bring the cavity back to resonance.

For a measurement of cavity length at time  $t$ , the mirror positions at  $t-\tau_1, t-\tau_2, \dots$ , are the retarded times for each mirror in reverse order around the beam path. The phase stability of the probe beam is assumed to be far better than the transit time. The following is a calculation for an equilateral triangle with two moving mirrors.

For the equilateral triangle shown in Figure 1, the mirror displacements are inward normal distances from equilibrium positions. These displacements are denoted as  $S_2$  and  $S_3$ . For

a cavity in equilibrium and on resonance,  $3 L_o = N_o \lambda_o$  with  $N_o$  representing the number of wavelengths. If the total cavity length changes and  $\lambda_o$  is changed to stay on resonance, then  $N_o$  stays the same.

The total optical path length of a cavity with moving mirrors can be constructed from Figure 2. The total optical path length  $L_T$  is given by

$$L_T = \left( L_o - \frac{S_2}{\cos \theta} \right) + \left( L_o - \frac{S_2}{\cos \theta} \cos 2\theta - \frac{S_3}{\cos \theta} \cos 2\theta \right) + \left( L_o - \frac{S_3}{\cos \theta} \right) \quad (2)$$

Using the identity,  $\cos 2\theta = 2 \cos^2 \theta - 1$ , equation (1) becomes

$$L_T = 3 L_o - 2 S_2 \cos \theta - 2 S_3 \cos \theta \quad (3)$$

where  $S_2$  and  $S_3$  are the instantaneous displacements when sampled by the optical wave. Expressing the optical path length in the clockwise direction as a function of time with  $\theta = 30^\circ$  yields

$$L_{T_{cw}} = 3 L_o - \sqrt{3} S_2 (t - \tau) - \sqrt{3} S_3 (t - 2\tau) \quad (4)$$

where,  $\tau = \frac{L_o}{c}$

Expressing the optical path length in the counterclockwise direction as a function of

time with  $\theta = 30^\circ$  yields

$$L_{T_{\text{exp}}} = 3 L_o - \sqrt{3} S_2 (t - 2\tau) - \sqrt{3} S_3 (t - \tau) \quad (5)$$

where,  $\tau = \frac{L_o}{c}$

The measurement time standard can be backed up by  $\tau$ , so that equations (3) and (4) become

$$L_{T_{\text{exp}}} = 3 L_o - \sqrt{3} S_2 (t) - \sqrt{3} S_3 (t - \tau) \quad (6)$$

$$L_{T_{\text{exp}}} = 3 L_o - \sqrt{3} S_2 (t - \tau) - \sqrt{3} S_3 (t) \quad (7)$$

The motion of the mirror is assumed to be sinusoidal with a frequency of  $\omega_d$  so that  $S_2(t)$  and  $S_3(t)$  are given by

$$S_2 (t) = A_2 \sin (\omega_d t) , \quad S_3 (t) = A_3 \sin (\omega_d t + \phi_3) \quad (7)$$

and

$$S_2 (t - \tau) = A_2 \sin [\omega_d (t - \tau)] , \quad S_3 (t - \tau) = A_3 \sin [\omega_d (t - \tau) + \phi_3] \quad (8)$$

where  $A_2$  and  $A_3$  are the amplitudes of the mirror motions and  $\phi_3$  is the phase difference between the motion of mirror 2 and mirror 3. Applying the trigonometric identity,  $\sin (\alpha - \beta) = \sin \alpha \cos \beta + \cos \alpha \sin \beta$ , yields

$$S_2 (t - \tau) \approx A_2 [\sin (\omega_d t) - (\omega_d \tau) \cos (\omega_d t)] \quad (10)$$

$$S_3 (t - \tau) \approx A_3 [\sin (\omega_d t + \phi_3) - (\omega_d \tau) \cos (\omega_d t + \phi_3)] \quad (11)$$

Substituting equations (7), (9) and (10) into equations (5) and (6) yields

$$L_{T_{cw}} = 3 L_o - \sqrt{3} [A_2 \sin(\omega_d t) + A_3 \sin(\omega_d t + \phi_3) - A_3 \omega_d \tau \cos(\omega_d t + \phi_3)] \quad (12)$$

$$L_{T_{ccw}} = 3 L_o - \sqrt{3} [A_2 \sin(\omega_d t) - A_3 \omega_d \tau \sin(\omega_d t + \phi_3) + A_3 \cos(\omega_d t + \phi_3)] \quad (13)$$

The difference in the effective cavity length between the clockwise and counterclockwise traveling laser beams is given by

$$\Delta L = L_{T_{cw}} - L_{T_{ccw}} = \sqrt{3} [A_3 \omega_d \tau \cos(\omega_d t + \phi_3) - A_2 \omega_d \tau \cos(\omega_d t)] \quad (14)$$

Operating under the condition that the clockwise and counterclockwise lengths separately are as stable as possible,  $A_3 = -A_2$ ,  $\phi_3 = 0$ . Then equation (13) becomes

$$\Delta L = -2 \sqrt{3} A_2 \omega_d \tau \cos(\omega_d t) \quad (15)$$

This change in frequency keeps the counter-propagating beams from locking together. This step has been achieved experimentally using mechanically vibrated mirrors. To remove the mechanical vibration completely, we can replace the mechanical motion of the mirrors using a Quantum Well Mirror (QWM) structure. A virtual reflecting surface can be moved back and forth (Figure 3) without physical motion of the mirror structure. This is accomplished by a multilayered quantum well optical filter. This effect is realized by modulating the index of refraction of key layers of the optical filter. The relative motion of the mirror surfaces is controlled so that the total optical path length around the RLG is held at a fixed value at all times. Although the path length is held constant, the relative motion of the mirrors causes an apparent rotation, which keeps the RLG out of lock-in.

The QWM structure consists of a quantum well optical filter made from alternating high and low index of refraction layers. The high index of refraction layers will be made of materials exhibiting the Stark effect in quantum wells at the operating wavelength of the RLG. The high and low index of refraction materials are deposited to form an optical edge filter. Deposited below the quantum well optical filter is a series of high and low index of refraction materials which form a highly reflective mirror structure (Figure 4). When the quantum well optical filter structure is not energized with an electric field, the structure is tuned to be an optical edge filter of high transmission (Figure 5). Therefore, the first reflection of the incident laser light occurs at the surface of the highly reflective mirror structure located below the quantum wells. When the quantum well optical filter is energized with an electric field, the structure becomes detuned and the first reflection of the incident laser light occurs at the top of the quantum well optical filter (Figure 6). An oscillatory signal applied to the quantum well structure will cause a non reciprocal phase modulation to the counter propagating laser beams in the cavity of an RLG.

### Material Selection

The III-V compounds, and in particular AlAs and  $\text{Al}_x\text{Ga}_{1-x}\text{As}$  were selected. These compounds form cubic crystals, zinc-blende arrangements at normal pressure. These crystals are also isotropic for crystal density, conductivity and refractive index. The lattice parameters are  $a_{\text{AlAs}} = 5.66139 \text{ \AA}$  and  $a_{\text{AlGaAs}} = 5.65330 + 0.00809x \text{ \AA}$  where  $x$  is the concentration of Al. These lattice constants allow for ideal growth conditions on a GaAs substrate whose lattice constant is  $a_{\text{GaAs}} = 5.65330$ . In addition the refractive index difference between  $\text{Al}_x\text{Ga}_{1-x}\text{As}/\text{AlAs}$  was significant enough to produce highly reflective mirrors with a reasonable amount of layered pairs. The Al concentration of the  $\text{Al}_x\text{Ga}_{1-x}\text{As}$  compound could also be adjusted to reduce the absorption of laser light to an acceptable level for RLG operation.



## Back Surface Mirror Structure

An analysis was performed to design a multi-layered  $\text{Al}_x\text{Ga}_{1-x}\text{As}/\text{AlAs}$  mirror using standard thin film techniques. The refractive indices for the III-V materials were selected based on the Al concentration needed to minimize absorption,  $>50\%$ . To achieve high reflectivity, a thin-film pair of alternating layers of high and low index of refraction  $\text{Al}_x\text{Ga}_{1-x}\text{As}/\text{AlAs}$  material was used in the design analysis. Each layer corresponded to an optical thickness of a quarter wavelength, with the wavelength set to  $6328 \text{ \AA}$ . This guarantees constructive interference for the reflected beam for maximum reflectivity. Based on the mirror analysis an  $\text{Al}_x\text{Ga}_{1-x}\text{As}/\text{AlAs}$  multi-layered stack of 55 layers was fabricated at Sandia National Laboratory. This semiconductor mirror was measured for reflectivity against a standard dielectric RLG mirror. The reflectivity of the semiconductor mirror was 0.7% better than the reflectivity of the dielectric RLG mirror. The calculated reflectivity for the semiconductor mirror was 99.97%. The semiconductor mirror was also placed in a V-cavity laser to determine if lasing would be produced (Figure 7). This was done to determine if the absorption losses were too great to sustain lasing. After a minor adjustment for alignment the cavity lased. It is expected that absorption loss was below the calculated 82 ppm. An additional loss in reflectivity and an increase in absorption loss also occurred because the top surface of the semiconductor mirror was coated with GaAs as a protective layer. A surface scan was also performed on the semiconductor mirror to determine its surface characteristics. The surface roughness was  $1.37 \text{ \AA rms}$  (Figure 8). This is slightly greater than the polished substrates used in the deposition of standard dielectric mirrors, typically  $<1.0 \text{ \AA rms}$ . The surface roughness represents the flatness of the cleaved unpolished substrate surface. The measurement of the scattering center produced a value of 92.3 (Figure 9). The scattering center scan provides a grade for the mirror which classifies the mirror as a C class mirror. An acceptable grade for an inertial instrument.

In reviewing the literature, several articles pertaining to the oxygenation of the AlAs

were obtained and reviewed. In reading these articles it was noted that oxygenation of the AlAs layer would drop its refractive index to 1.6 from 3.14. This large change in the index would allow the fabrication of the mirror to be performed in 15 to 20 layered pairs with a higher reflectivity than produced by the current design 99.99981% (Figure 10).

### Quantum Well Superlattice for QWM

An  $\text{Al}_x\text{Ga}_{1-x}\text{As}/\text{AlAs}$  superlattice structure was designed and fabricated as a first step in determining the ability of the quantum well superlattice to provide the characteristics needed to operate as a front surface filter. The device was fabricated by Lucent Technology using Molecular Beam Epitaxy (MBE). The structure is currently being patterned in order to experimentally evaluate the magnitude of the Stark shift, and its transmission, reflectance, and absorption properties. The surface of the quantum well superlattice was initially surfaced scanned after fabrication to determine its suitability as a mirror for gyroscope operation since the beam is reflected off the front surface when the filter is operational. Surface flatness was measured followed by a measurement of scattering centers per unit area. The surface flatness was 2.67 Å rms (Figure 11) and the scattering center number was 164.2. As previously discussed the surface flatness and scattering center numbers provide a means of determining the suitability of the device for mirror application in an RLG. The 2.67 Å rms surface flatness number is the flatness produced by the properties of the substrate. The substrate was an off the shelf item chemically cleaned before depositing the materials. The scattering center number is a relative number and helps to designate a class of mirrors. An RLG with a scattering center number of 164.2 will have a lock-in band of  $\approx 1600$  deg/hr. This number does not present a serious problem because the dither frequency of the QWM is in the 100's of megahertz. The contribution to the random wander due the dither is effectively reduced by 541. The dither contribution is proportional to the lock-in frequency and inversely proportional to the dither drive frequency (see Equation 1). It is expected that the scattering center number was high because the substrate was of a lesser quality.

In addition to the experimental work to measure the magnitude of the Stark shift, and the transmission, reflectance, and absorption properties of the superlattice the manufacturability of this device will also be determined. This will be achieved because the pattern etched on the wafer for the experimental work will be in a matrix form (Figure 13). Each structure on the wafer can be selected for optical characterization, as the information is obtained it will also provide information on the optical characteristics as a function of position on the wafer. This will provide information on the yield per wafer. This is needed because the QWM structures take up a larger amount of surface area than typical electronic components. This is due to the beam size.

### **Amplitude of Drive Oscillations**

A calculation was also performed to determine how to decouple the forward and backscattered components of the two primary beams in the RLG cavity. The analysis showed that the forward component can be reduced to zero if the argument of the zero order Bessel function can be driven to zero. The back-scattered component was reduced by the dither drive amplitude. The higher the drive frequency, the lower the back-scattered component. This analysis also provided the amount of movement required to drive the QWM for biasing. The calculated distance was less than a wavelength.

### **Current and Future Efforts**

Currently, work is continuing on the design of the filter for the QWM. It is expected that the filter will be designed by mid-June with fabrication and evaluation to follow. The structure will be evaluated for its surface characteristics, reflection, absorption and its ability to shift the reflecting plane. After several cycles of design optimization, that is, of design, fabrication, and evaluation of the filter a QWM will be designed. Consideration will be given to key RLG parameter in order to achieve the required phase shift. During the QWM development, cycle, and after internal evaluation of the QWM structures, structures

will be given to RLG manufacturers for evaluation. Based on the feedback from these manufacturers, modification will be made to tailor the component for RLG operation. A test and evaluation period will be performed with QWM's in RLG'S. Based on the results of the test and evaluation period additional modifications will be made to the QWM's. Transition will occur only after complete design optimization of the QWM for the RLG has been performed.

### **Acknowledgements**

The authors of this paper would like to thank the Office of Naval Research, Wright Patterson Airforce Base Avionics Division, and Eglin Airforce Base WCMD group for their program support. In addition, we would like to thank Kearfott Guidance and Navigation Company , Honeywell and Sandia National Laboratory for cooperation in the development and evaluation of structures for the program.

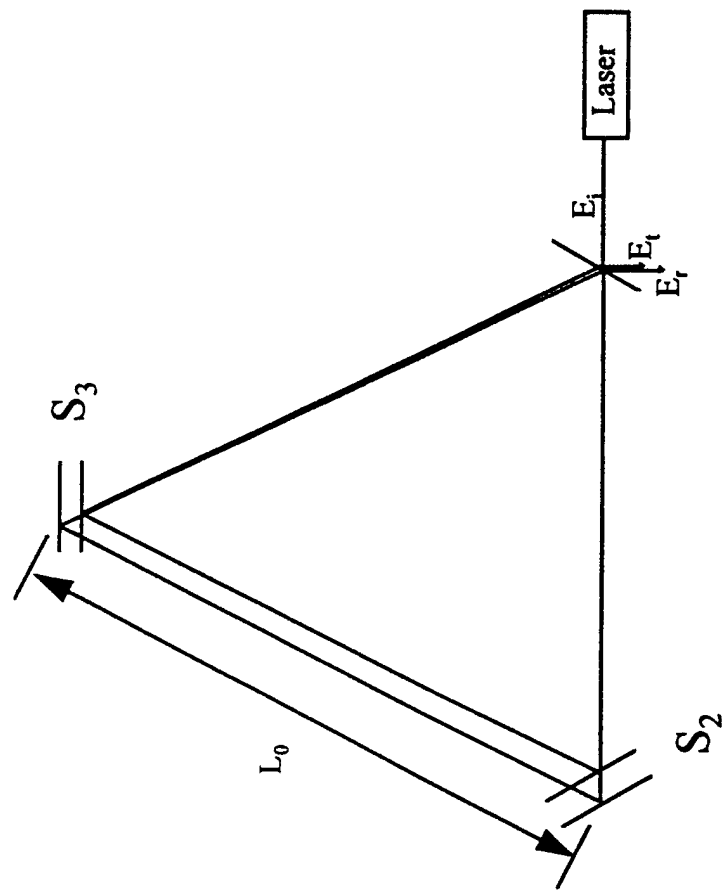


Figure 1 Simple Example of Mirror Motion

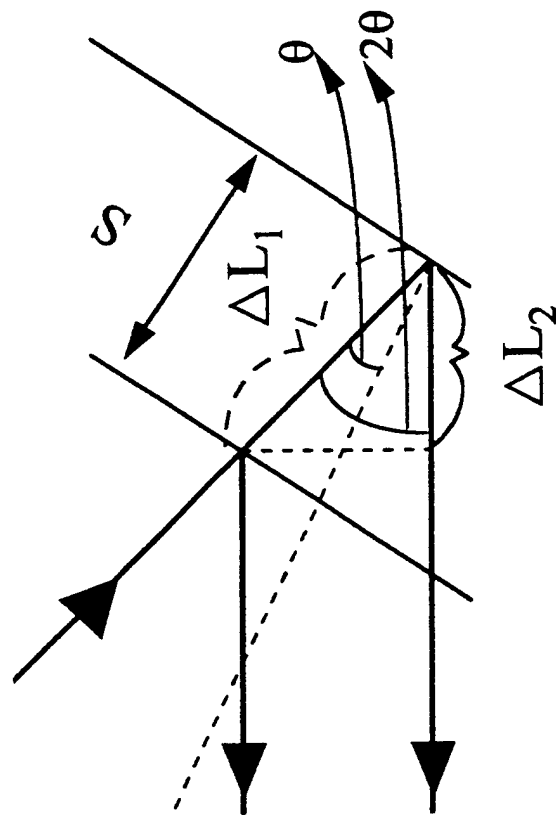


Figure 2: Mirror Movement

Electrode
QW
L
QW
L
QW
Electrode
AlAs
AlGaAs
AlAs
AlGaAs
AlAs
Substrate

Figure 4: Multilayered Quantum Well Optical Filter with Mirror

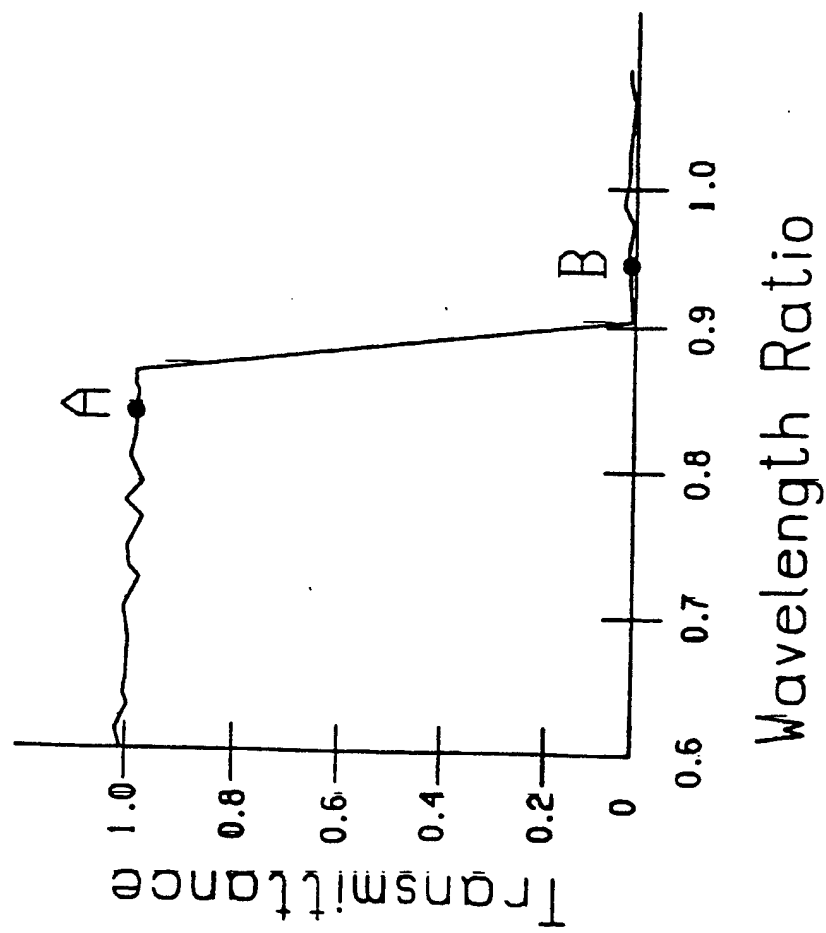


Figure 5: Filter Response



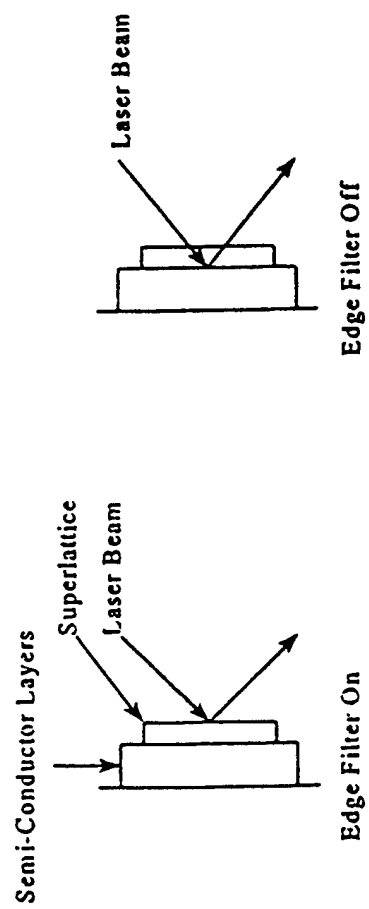


Figure 6: Filter Response



Figure 7: Semiconductor Mirror in a V-Cavity Laser

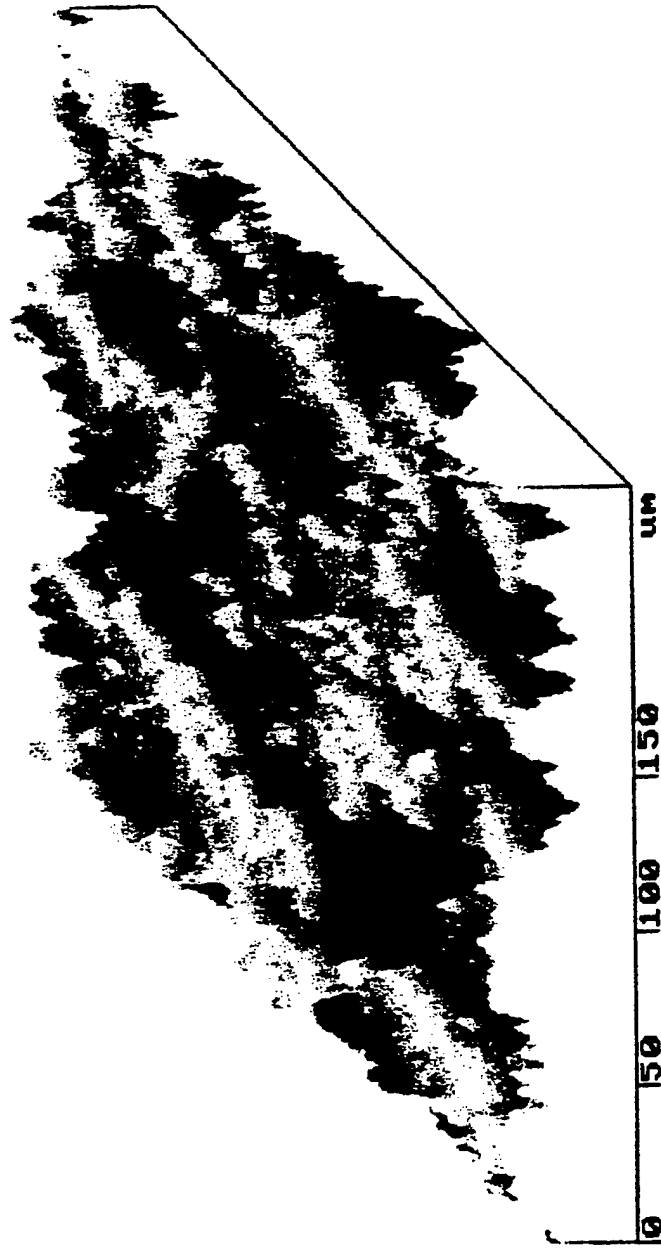


Figure 8: Surface Scan of a Semiconductor Mirror

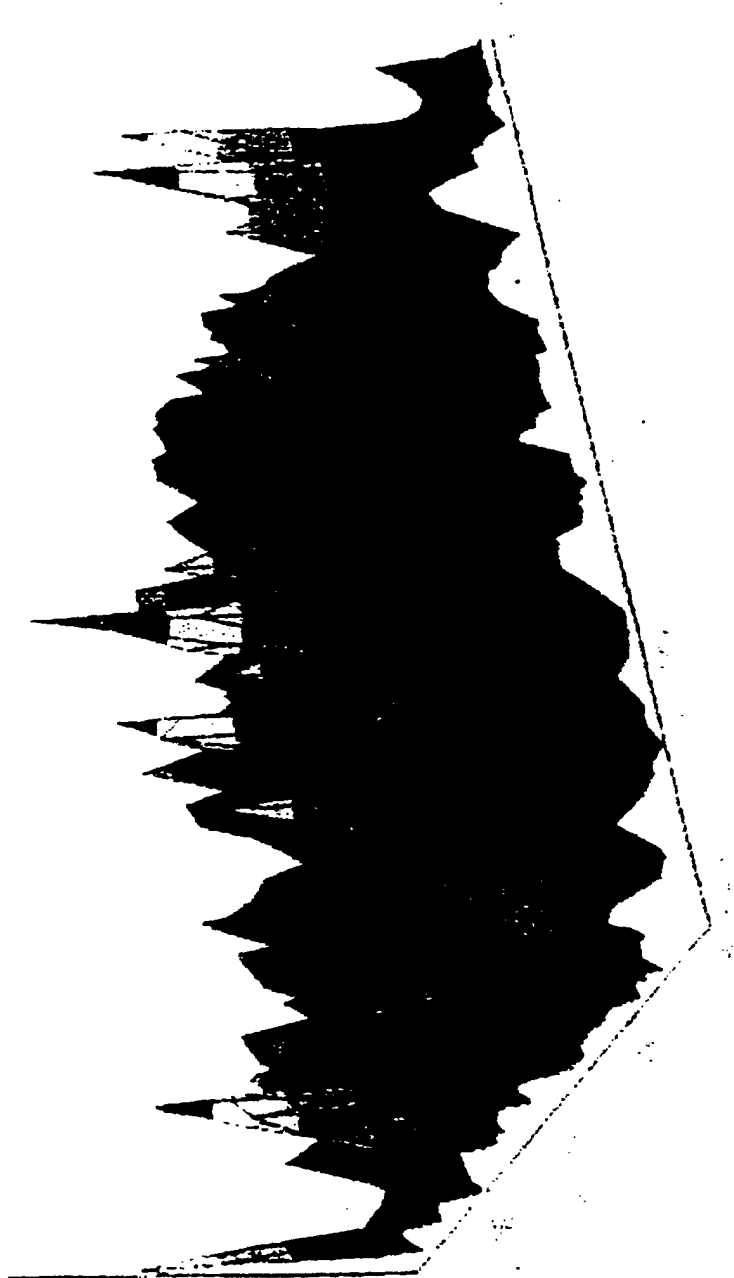


Figure 9: Scattermeter Measurement of a Semiconductor Mirror

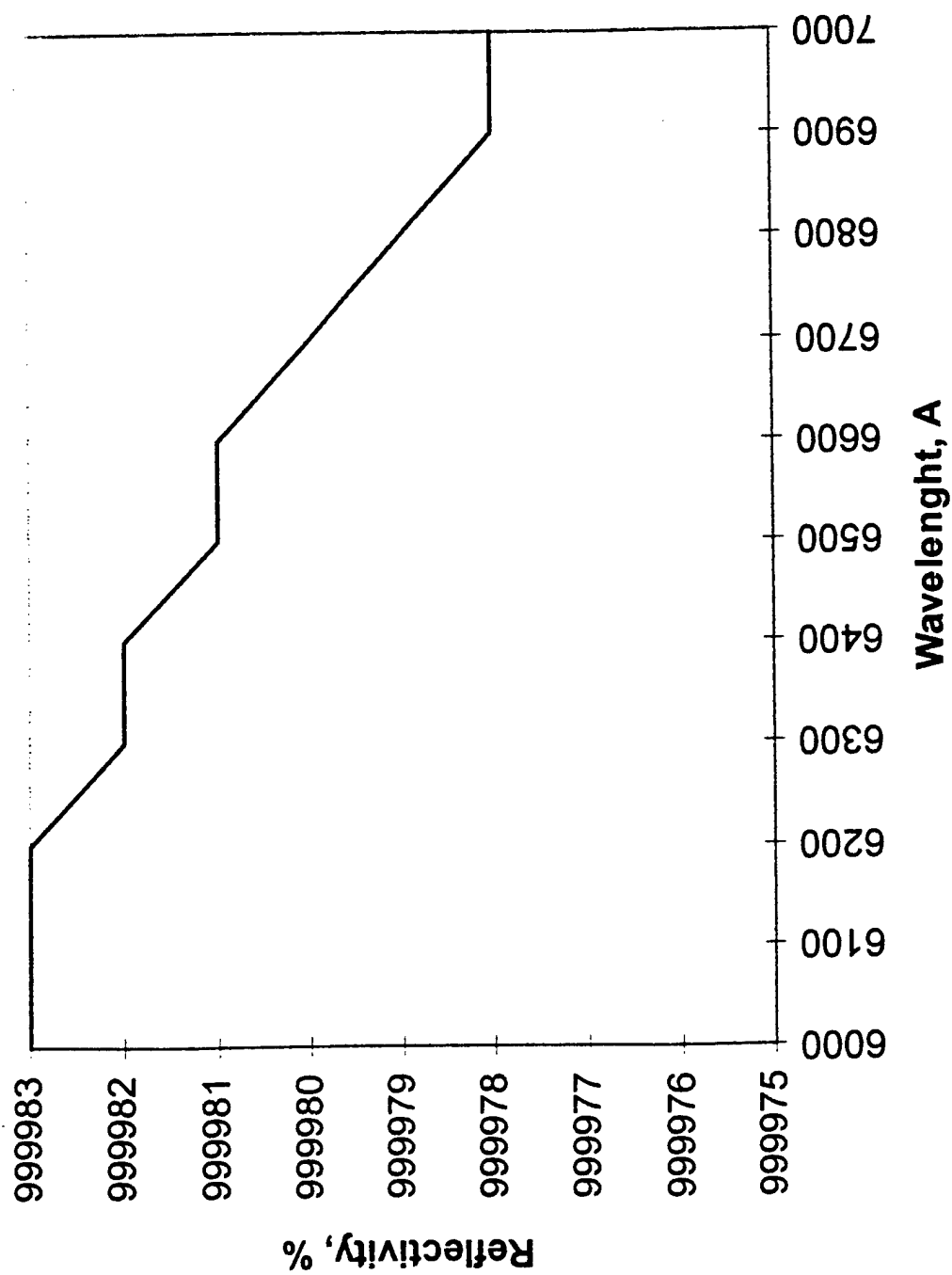


Figure 10: Oxygenated Semiconductor Mirror. 30 Degrees Incidence

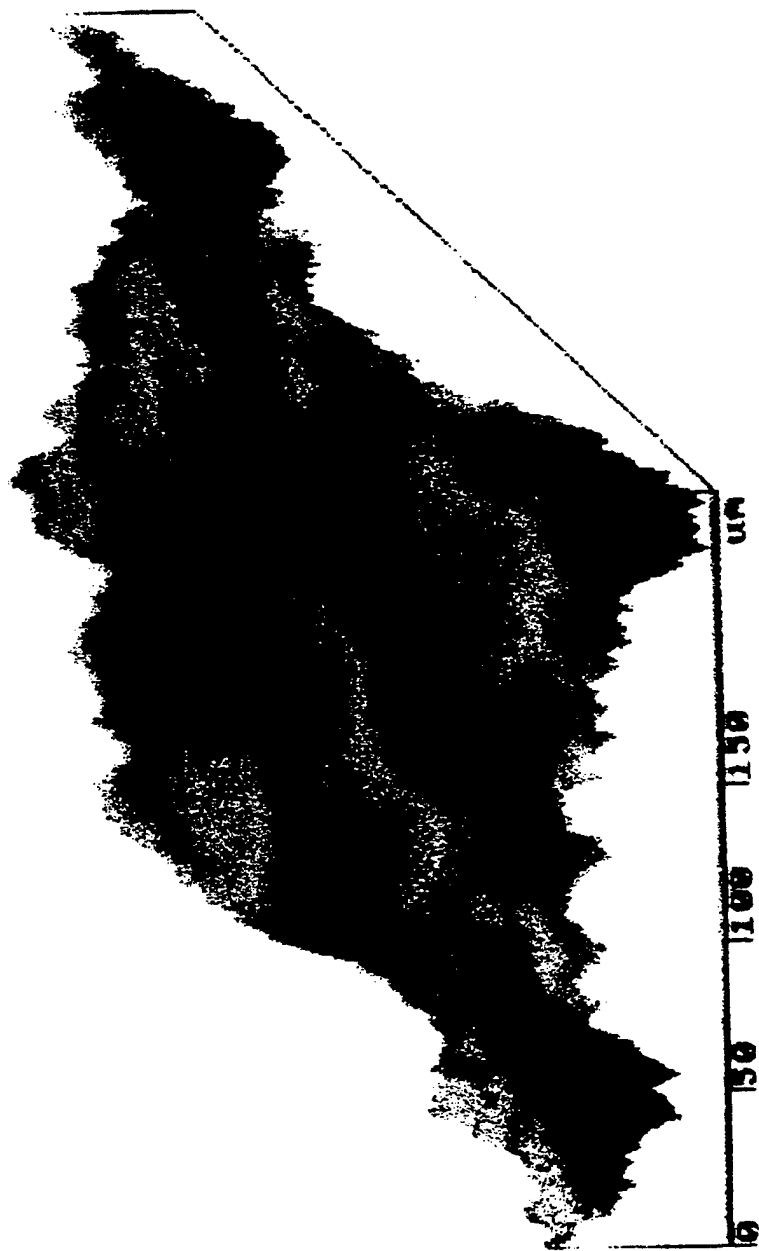


Figure 11: Surface Scan Quantum Well Superlattice

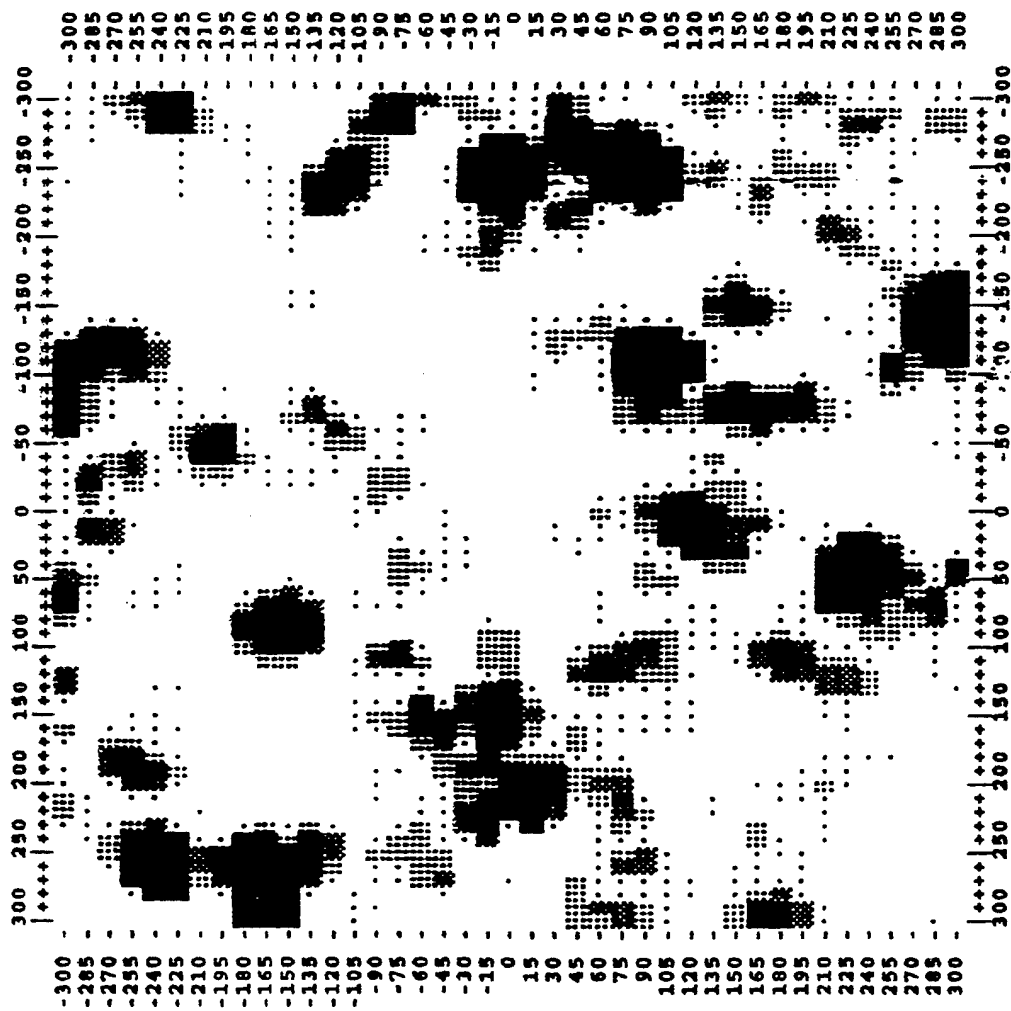


Figure 12: Scattermeter Measurement of a Quantum Well Superlattice

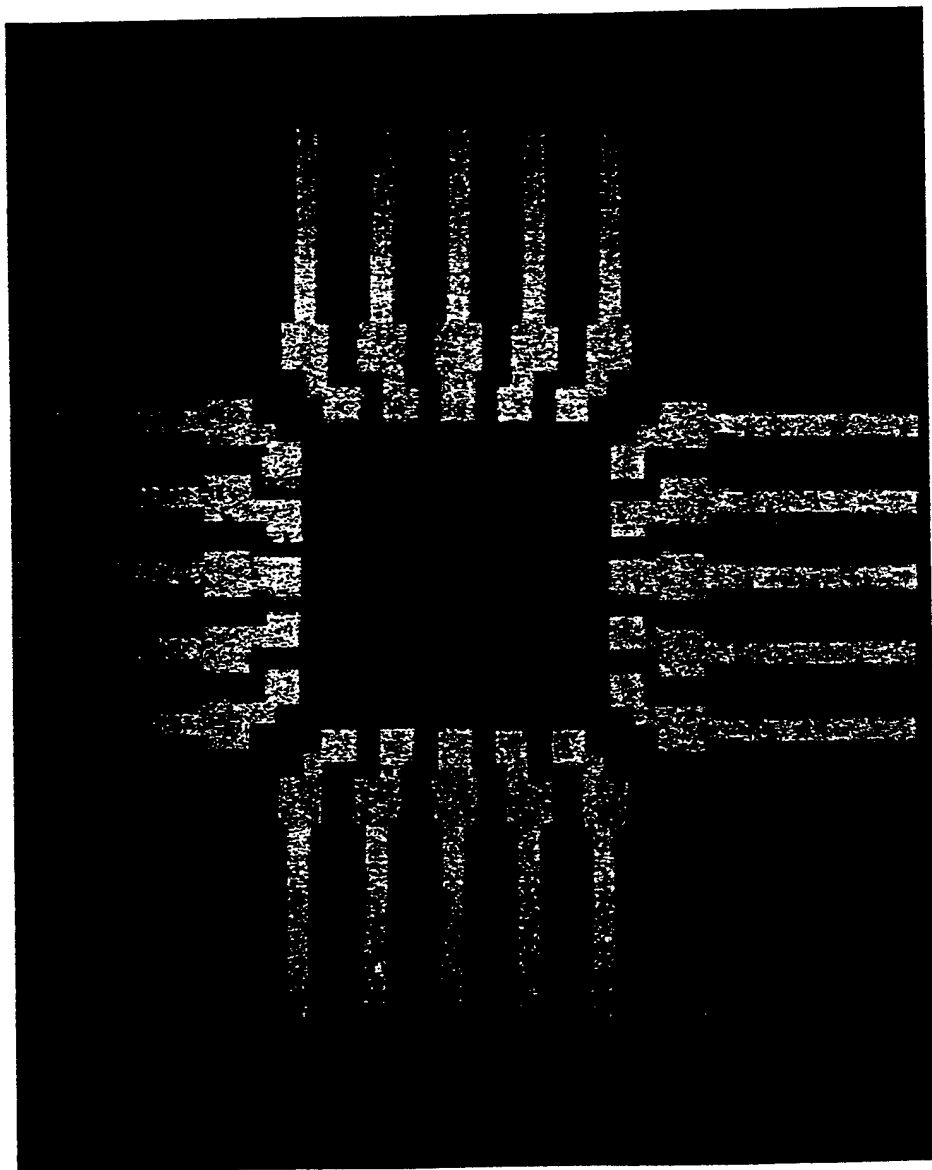


Figure 13: Quantum Well Superlattice Etched Wafer